

## Ultrafine particles of North Sea illite/smectite clay minerals investigated by STM and AFM

**HOLGER LINDGREEN**

Clay Mineralogical Laboratory, Geological Survey of Denmark, Thoravej 8, DK 2400, Copenhagen NV, Denmark

**JØRGEN GARNÆS\***

Department of Physics, University of California, Santa Barbara, California 93106, U.S.A.

**POUL L. HANSEN**

Laboratory of Applied Physics, Technical University of Denmark, DK 2800 Lyngby, Denmark

**FLEMMING BESENBACHER, ERIK LÆGSGAARD, IVAN STENSGAARD**

Institute of Physics, University of Aarhus, DK 8000 Aarhus C, Denmark

**SCOT A. C. GOULD, PAUL K. HANSMA**

Department of Physics, University of California, Santa Barbara, California 93106, U.S.A.

### ABSTRACT

We have applied scanning tunneling microscopy (STM) and atomic force microscopy (AFM) to study particle shape and thickness in illite/smectite (I/S) from the North Sea Jurassic oil source rocks. We demonstrate that STM can be used on our I/S particles, despite their poor conductivity, if they are ultrathin ( $\sim 10$  Å) and, furthermore, that detailed surface topography of our I/S particles can be mapped by STM and AFM and even at the atomic resolution level by AFM. The accurate thickness measurements show that our material contains lath-shaped particles 10 Å thick, which are elementary smectite particles according to the fundamental particle concept but can be both smectite and mica (illite) according to the AIPEA classification. Surface adsorbed layers, probably of H<sub>2</sub>O, can be seen in STM images of I/S particles that previously were cleaned for organic compounds and iron and aluminum oxides. On I/S particles, STM and AFM give data that hitherto have not been obtained by other methods and that provide insight into clay mineral diagenetic processes and into adsorption on clay mineral surfaces.

### INTRODUCTION

Mixed-layer illite/smectite (I/S) is one of the most abundant clay minerals in nature (Weaver, 1988), and the increase in the proportion of illite layers in I/S during sediment diagenesis, especially during oil formation in oil field source rocks, has been extensively studied (Perry and Hower, 1970; Hower et al., 1976; Foscolos et al., 1976; Bruce, 1984; Glasmann et al., 1989). Until now, thicknesses of I/S particles have been calculated predominantly from the length of their shadow cast at a low angle in Pt-shadowed specimens for transmission electron microscopy (TEM). Thickness data thus obtained led to the fundamental particle concept for the structure of I/S (Nadeau et al., 1984) and to the development of a smectite dissolution–illite crystallization model for formation of illite layers in I/S (Nadeau et al., 1985). TEM thickness measurements have also been used to distinguish between particles of smectite (10 Å thick) and illite (20 Å thick or more) (Glasmann et al., 1989). However, the low

accuracy ( $\pm 4$  Å at a shadowing angle of 10°, Nadeau et al., 1987) of particle thickness measurements in shadowed TEM specimens limits the significance of these data.

Previously, we have investigated about 50 samples of Upper Jurassic shale from oil wells in the Danish and Norwegian concession areas by X-ray diffraction (XRD), high resolution transmission electron microscopy (HRTEM), and TEM (Hansen and Lindgreen, 1989). In the present paper, we report STM and AFM investigations on two of these samples, from a depth of 3365 m in well 2/7-3 in the Eldfisk Field and from a depth of 4548 m in well 2/11-1 in the Valhall Field, both in the Ekofisk Field complex. Upper Jurassic shales are the most important source rocks for the North Sea oil (Barnard and Cooper, 1981), and I/S is present in large amounts in these rocks.

### STRUCTURE MODELS FOR ILLITE/SMECTITE

Mixed-layer I/S is assumed by the Markov theory to consist of thick (5–15 layers of 10 Å thickness) MacEwan particles with smectite and illite layers (Reynolds, 1984) and by the fundamental particle theory (Nadeau et al., 1984) to consist of thin particles (elementary smectite

\* Present address: Danish Space Research Institute, Gl. Lundtoftevej 7, DK 2800 Lyngby, Denmark.

particles 10 Å thick and illite particles 20 Å and thicker, Nadeau et al., 1984, 1985). In such a mixture of fundamental particles, I/S XRD patterns should result from interparticle diffraction (Nadeau et al., 1984): smectite XRD spacings result from one smectite layer 10 Å thick plus one interparticle spacing or one particle-terminating illite layer (10 Å) plus one interparticle spacing, whereas the illite XRD spacings result from illite layers 10 Å thick (Nadeau et al., 1984). The Markov theory for I/S was based on XRD of thick specimens prepared from dispersed I/S, whereas the fundamental particle theory was based on XRD in combination with particle thickness measurements by TEM on shadowed specimens also prepared from dispersed I/S. Later, HRTEM has shown that, in intact bulk rock, I/S is present as MacEwan particles (Ahn and Peacor, 1986; Hansen and Lindgreen, 1987, 1989; Ahn and Buseck, 1990; Lindgreen and Hansen, 1991) and that the dispersion procedures are responsible for the formation of the thin, fundamental particles seen by TEM in dispersed I/S.

#### MINERALOGICAL DATA FOR THE INVESTIGATED ILLITE/SMECTITE

Comparison of experimental XRD patterns and those obtained by computer simulation by the Newmod program of R. C. Reynolds showed that the I/S from well 2/7-3 (3365 m) contains 60% smectite layers and is R0 ordered and that the I/S from well 2/11-1 (4548 m) contains 15% smectite layers and is IS ordered (Lindgreen and Hansen, 1991). (R0 ordering means that illite and smectite layers in I/S are randomly distributed, whereas IS ordering means that a layer of the minor component is always followed by at least one layer of the major component in the I/S sequence of layers.) Particle thicknesses were calculated from TEM micrographs of shadowed I/S from the lengths of the shadows. I/S particles from well 2/7-3 (3365 m) are largely 10 Å thick (70%) and 20 Å thick (20%), and I/S particles from well 2/11-1 (4548 m) are about equally (~20%) 20, 30, 40, 50, and 60 Å thick (Lindgreen and Hansen, 1991).

Lath-shaped particles are abundant in the I/S from well 2/7-3 (3365 m), and their thicknesses are, from the TEM measurements, predominantly 10 Å. These particles are thus elementary smectite particles according to the fundamental particle concept (Nadeau et al., 1984). Lath-shaped smectite particles were present in large proportions in Upper Jurassic sediments in the Atlantic Ocean (Holtzapffel and Chamley, 1986) and have probably formed by dissolution and crystallization in the sediments (Holtzapffel and Chamley, 1986). However, accurate thicknesses of the lath-shaped particles have so far not been determined.

#### EXPERIMENTAL DATA

The AFM (Binnig et al., 1986) gives topographic images by scanning a sharp tip over a surface (Hansma et al., 1988) and has been used to produce atomic resolution images of both conductors (Binnig et al., 1987) and non-

conductors (Albrecht and Quate, 1987; Drake et al., 1989). The STM records electron tunneling between a sharp metal tip and a conducting surface and thereby gives information on the electronic and geometrical structure of semiconductor and metal surfaces (Binnig and Rohrer, 1986; Hansma and Tersoff, 1987). We have used the superior resolving power of STM and AFM to investigate I/S. The use of STM should seem impossible since clay minerals are in general poor conductors. We were, however, able to obtain tunneling conditions during investigation of isolated, very thin (10 Å–30 Å) I/S particles on freshly cleaved HOPG (highly oriented pyrolytic graphite). Although the exact mechanism is not well understood, tunneling through thin insulating objects has previously been observed and utilized in several cases, mainly in the field of biology (Hansma et al., 1988; Engel, 1991). In mica crystals, electrical conduction can take place by polaron hopping between Fe<sup>3+</sup> sites in mica crystals, and conductivity measurements on mica have to be carried out on samples >50 Å thick to prevent tunneling between electrodes (Meunier et al., 1983). This agrees with our finding of tunneling in ultrathin particles of I/S from well 2/7-3, 3365 m, which has a total Fe content of 5.9% Fe<sub>2</sub>O<sub>3</sub> and a Fe<sup>2+</sup>/Fe<sup>3+</sup> ratio of 0.25 (Lindgreen et al., 1991).

Our samples were cleaned of organic matter and iron and aluminum oxide coatings, and after dispersion, I/S was isolated by centrifugation (Hansen and Lindgreen, 1989).

The specimens with isolated particles were obtained by leaving a drop of 0.2 mg Na<sup>+</sup>-saturated I/S in 1 mL distilled H<sub>2</sub>O to dry on a mineral surface, on HOPG for STM, and on freshly cleaved mica for AFM. This low concentration of I/S is essential for achieving high resolution images. For STM, we have taken advantage of a new high-stability, fully automated Tunnelscope 2400 from Struers (Lægsgaard et al., 1989). The experiments were performed in ambient air with electrochemically etched Pt-Ir tips. The sample bias was -181 mV and the tunneling current 0.5 nA. The dimensions of the images were calibrated from the atomic structure of the graphite (Lægsgaard et al., 1989), which was clearly resolved at all sides of the clay particles. The substrate was scanned extensively to rule out any confusion with surface defects that have quite a different character. For AFM, we used a Nanoscope II Force microscope from Digital Instruments (Santa Barbara, California) that was calibrated with the mica lattice. It worked routinely and was ideally suited to those measurements.

#### PARTICLE THICKNESSES

The particle thicknesses calculated from shadow lengths in TEM photos and used so far (Glasmann et al., 1989; Nadeau et al., 1984, 1985; Eberl et al., 1987) are only accurate within ±4 Å (Nadeau et al., 1987) at most, and it may be difficult to detect them if the particles are lying flat on the surface or rest on other particles. Particles can, however, be scanned accurately by STM and AFM. The thickness plots in Figures 1 and 2 show that the lath-

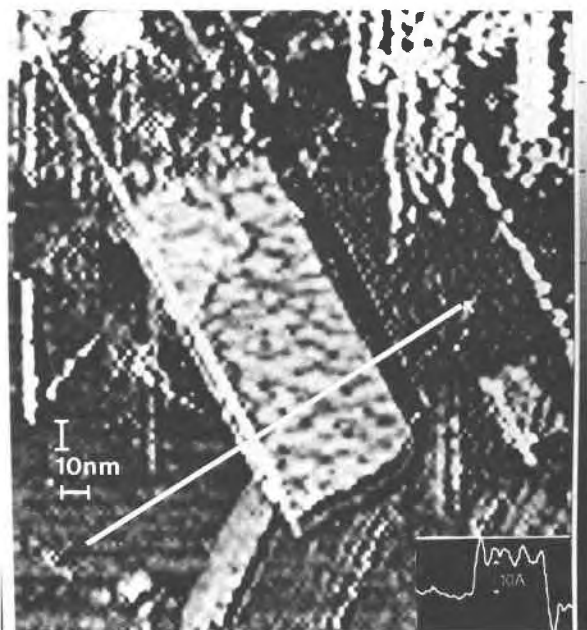


Fig. 1. Scanning tunneling microscope image of lath-shaped particle in illite/smectite from well 2/7-3 (3365 m), with profile of the particle along the line shown in the top view. The particle is a single layer of 10 Å thick, probably a smectite particle.

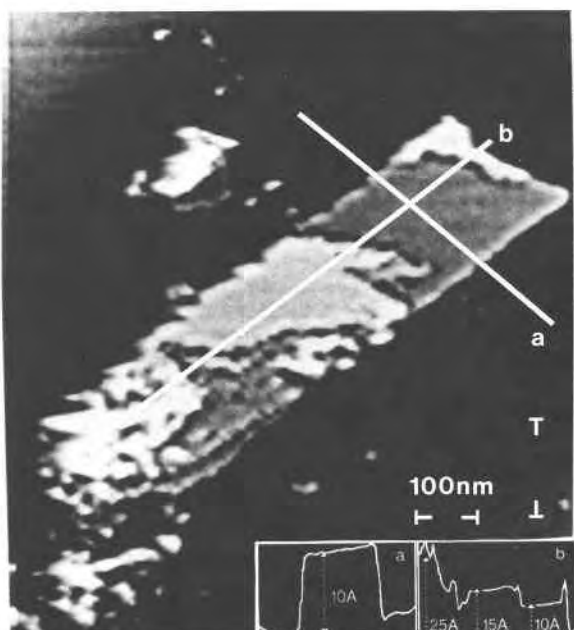


Fig. 2. Scanning tunneling microscope image of lath-shaped particle in illite/smectite from well 2/7-3 (3365 m), with profiles of the particle along lines a and b. The particle consists of a single layer 10 Å thick (probably smectite) partially superimposed by minor layers of variable thickness, which may be adsorbed H<sub>2</sub>O.

shaped particles are 10 Å thick. The accuracy of thickness measurements on poorly conducting material cannot be determined from the accuracy obtained from the conducting graphite support. The thickness of 10 Å for part of the particle in Figure 2 (profile a) corresponds well to the thickness of a 2:1 silicate layer (9.3–9.5 Å) and  $d(001)$  of muscovite of 10.0–10.3 Å (Bailey, 1984). The accurate STM data therefore confirm the data from shadowed TEM pictures, i.e., the lath-shaped particles in our samples are elementary smectite particles according to the fundamental particle concept (Nadeau et al., 1984). The fundamental particle concept (Nadeau et al., 1984) used the term illite and used the thickness of particles as a classification criteria, whereas the AIPEA classification (Bailey, 1980) used the term mica and used the amount of charge in the layers as a classification criteria, mica having a charge of  $-1.0$  per  $O_{10}(OH)_2$  and smectite a charge of  $-0.2$  to  $-0.6$  per  $O_{10}(OH)_2$  (Bailey, 1980). Because of their high charge, mica (or illite) layers should be able to dehydrate and fix K between layers (Eberl, 1986) to form 20 Å or thicker particles. Smectite layers should, because of their lower charge, be able to remain single layered in dispersed I/S. We cannot, however, exclude the possibility that single layers of mica (after the AIPEA classification) exist and that some of the 10 Å particles in Figures 1 and 2 and in previous investigations (Nadeau et al., 1984, 1985) are mica (or illite, if that term is used).

#### SURFACE CHARACTERIZATION

The particle in Figure 1 has steps of approximately 4 Å on the surface. Na<sup>+</sup>-saturated smectite has, from XRD

determinations of basal spacings, one layer ( $\sim 2.5$  Å thick) of H<sub>2</sub>O molecules at relative humidities of 0.1–0.5, one to two layers at 0.5–0.7, and two layers ( $\sim 5$  Å thick) at 0.5–0.9 relative humidity (Glaeser and Méring, 1968). In our STM laboratory, the humidity was  $\sim 0.7$ . The steps on the particle in Figure 1 may therefore well be H<sub>2</sub>O adsorbed around the Na<sup>+</sup> cations. The particle in Figure 2 has irregularly shaped surface coatings. These cannot be organic matter or oxides of Fe or Al, as these have been removed by chemical pretreatment, but may be one or more layers of adsorbed H<sub>2</sub>O. Part of the particle has an even surface corresponding to 10 Å particle thickness, the thickness of the 2:1 clay mineral layer, and thus has not adsorbed H<sub>2</sub>O. Adsorption (or eventually fixation) of cations and H<sub>2</sub>O molecules on clay surfaces results from the negative layer charge arising from substitutions in the 2:1 layer. If the surface coatings are adsorbed H<sub>2</sub>O then the particle in Figure 1 could well have an even distribution of charge, whereas the particle in Figure 2 has an uneven distribution of charge. Previous data for H<sub>2</sub>O adsorption on layer silicates (Glaeser and Méring, 1968) are average values per layer, and STM provides the possibility for new insight in H<sub>2</sub>O adsorption and its localization on single sheet surfaces of clay minerals.

The insulating properties of clay minerals do not permit STM to be used on thicker particles, but these can be examined by atomic force microscopy (Figs. 3 and 4). A particle  $\sim 70$  Å thick from the I/S in well 2/11-1 (4548

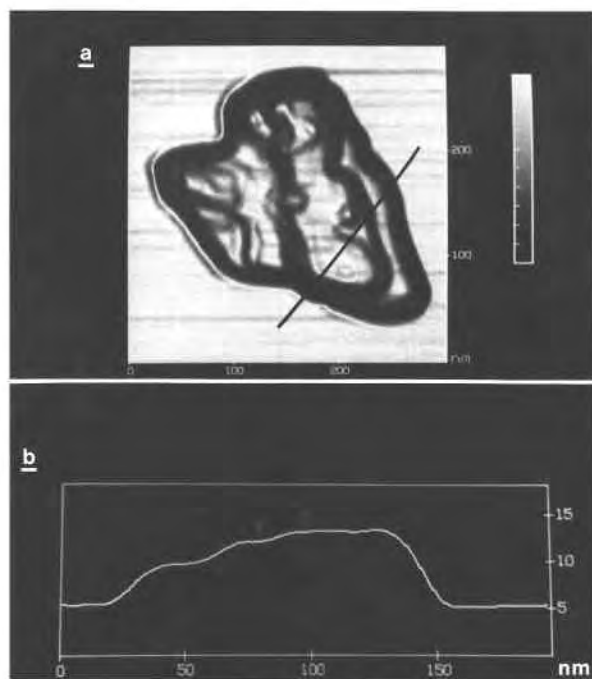


Fig. 3. (a) Atomic force microscope image of a particle from illite/smectite from well 2/11-1 (4548 m). The image shows a thick particle with an area of  $\sim 0.05 \mu\text{m}^2$ . (b) Profile of the particle in a along the line shown in the top view. The particle is  $\sim 70 \text{ \AA}$  high and has one step markers of  $\sim 10 \text{ \AA}$  on the top.

m) is shown in Figure 3. A  $10 \text{ \AA}$  step is, from the profile, present on the surface. The picture in Figure 4 shows high-resolution AFM of the surface of the particle in Figure 3. Recently, AFM resolution at unit-cell level on standard illite and smectite minerals was achieved (Hartman et al., 1990). A Fourier transform of the raw data in Figure 4a showed two lattice spacings of  $4.5$  and  $2.6 \text{ \AA}$ , with a relative angle of  $30^\circ$ . The  $5.2 \text{ \AA}$  distance between large minima in Figure 4 corresponds to the unit-cell resolution of  $5 \text{ \AA}$  seen before (Hartman et al., 1990), whereas the  $2.6 \text{ \AA}$  period corresponds to the O-O distance in the O hexagons of the tetrahedral sheet. Highly resolved STM images of thin particles also revealed  $5$  and  $2.6 \text{ \AA}$  periods. The contours on the surface (Fig. 4) could thus represent the hexagonal O surface of the tetrahedral sheet of the 2:1 layer if some tetrahedra were tilted slightly to bring some O atoms slightly out of the plane. Figure 4 would then be the first atomic resolution image of a silicate surface. According to the image, however, the hexagonal holes are empty. This suggests that the scanning tip pushes interlayer cations out of the holes. This could easily happen for the adsorbed, hydrated cations (in our samples  $\text{Na}_{\text{aq}}^+$ ) but is less likely for fixed, dehydrated cations ( $\text{K}^+$  or  $\text{NH}_4^+$ ). Fixed, dehydrated  $\text{K}^+$  or  $\text{NH}_4^+$  may, however, not be present in this top tetrahedral sheet. An alternative explanation for the contours in Figure 4 is that the contours represent the  $\text{H}_2\text{O}$  layers adsorbed on the clay min-

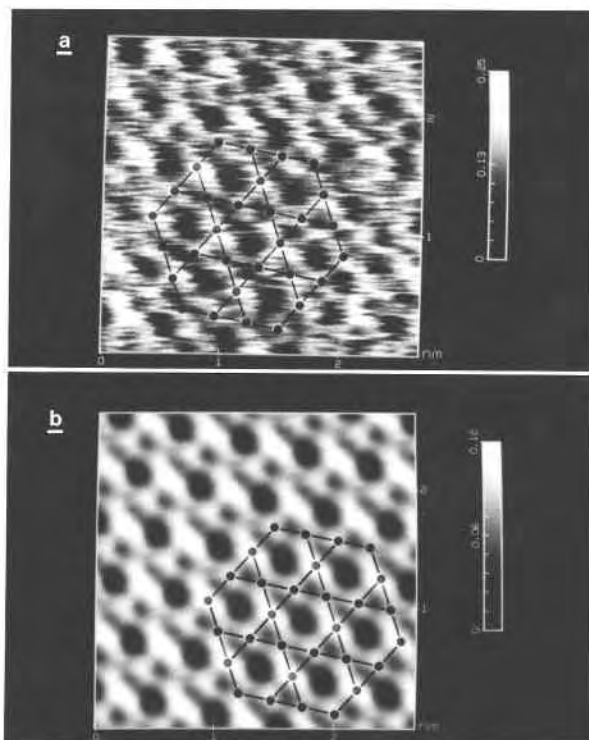


Fig. 4. Atomic force microscope image of the surface of the particle in Figure 3. (a) Raw data (except for slight low-pass filtering during data acquisition). (b) Processed data obtained by unit-cell averaging over more than 50 unit cells. The inserted model shows the arrangement of O atoms on the surface of the tetrahedral sheet. The scan area is  $2.6 \times 2.6 \text{ nm}$ .

eral surface. Both the recent investigation (Hartman et al., 1990) and our experiments were carried out at relative humidities at  $50$ – $80\%$ , where  $1$ – $2$  layers of  $\text{H}_2\text{O}$  are adsorbed on clay mineral surfaces. It has been suggested that the silicate surface acts as a template for the adsorbed  $\text{H}_2\text{O}$  molecules (Davidtz and Low, 1970; Ravina and Low, 1972, 1977). The raw data in Figure 4a show rather irregular contours, as such a layer adsorbed on the silicate surface should have. We believe that the image in Figure 4 shows the O hexagons of the surface of the tetrahedral sheet but cannot exclude that it is an image of the surface of the first or second layers of adsorbed  $\text{H}_2\text{O}$ .

## CONCLUSIONS

We conclude that STM and AFM has given accurate three-dimensional data for ultrafine clay particles and that AFM has provided information about the structure of the surface of the 2:1 layer. In the future, AFM and STM can be used to study the atomic structure of clay minerals and the adsorption of molecules on their surfaces.

## ACKNOWLEDGMENTS

We thank S. Manne for useful discussions. The AFM work was supported in part by the Office of Naval Research and Digital Instruments. The STM work was supported by the Knud Højgaard Foundation. One

of the authors (J.G.) wishes to acknowledge the support of the Danish Research Academy, the Danish Space Research Institute, and Danish Micro Engineering A/S.

### REFERENCES CITED

- Ahn, J.H., and Buseck, P.R. (1990) Layer-stacking sequences and structural disorder in mixed-layer illite/smectite: Image simulations and HRTEM imaging. *American Mineralogist*, 75, 267–275.
- Ahn, J.H., and Peacor, D.R. (1986) Transmission electron microscope data for rectorite: Implications for the origin and structure of "fundamental particles." *Clays and Clay Minerals*, 34, 180–186.
- Albrecht, T.R., and Quate, C.F. (1987) Atomic resolution imaging of a nonconductor by atomic force microscopy. *Journal of Applied Physics*, 62, 2599–2602.
- Bailey, S.W. (1980) Summary of recommendations of AIPEA nomenclature. *Clays and Clay Minerals*, 28, 73–78.
- (1984) Structures of layer silicates. In G.W. Brindley and G. Brown, Eds., *Crystal structures of clay minerals and their X-ray identification*, p. 1–124. Mineralogical Society, London.
- Barnard, P.C., and Cooper, B.S. (1981) Oils and source rocks of the North Sea area. In L.V. Illing and G.D. Hobson, Eds., *Petroleum geology of the continental shelf of north-west Europe*, p. 169–175. Heyden and Son, London.
- Binnig, G., and Rohrer, H. (1986) Scanning tunnel microscopy. *IBM Journal of Research and Development*, 30, 355–369.
- Binnig, G., Quate, C.F., and Gerber, C. (1986) Atomic force microscope. *Physics Review Letters*, 56, 930–933.
- Binnig, G., Gerber, C., Stoll, E., Albrecht, T., and Quate, C.F. (1987) Atomic resolution with atomic force microscope. *Europhysics Letters*, 3, 1281–1287.
- Bruce, C.M. (1984) Smectite dehydration—Its relation to structural development and hydrocarbon accumulation in Northern Gulf of Mexico Basin. *American Association of Petroleum Geologists Bulletin*, 68, 673–683.
- Davidtz, J.C., and Low, P.F. (1970) Relation between crystal-lattice configuration and swelling of montmorillonites. *Clays and Clay Minerals*, 18, 325–333.
- Drake, B., Prater, C.B., Weisenhorn, A.L., Gould, S.A.C., Albrecht, T.R., Quate, C.F., Cannell, D.S., Hansma, H.G., and Hansma, P.K. (1989) Imaging crystals, polymers, and processes in water with the atomic force microscope. *Science*, 243, 1586–1589.
- Eberl, D. (1986) Sodium-potassium ion exchange during smectite diagenesis—A theoretical discussion. *U.S. Geological Survey Bulletin*, 1578, 363–368.
- Eberl, D.D., Śródoń, J., Lee, M., Nadeau, P.H., and Northrop, H.R. (1987) Sericite from the Silverton caldera, Colorado: Correlation among structure, composition, origin, and particle thickness. *American Mineralogist*, 72, 914–934.
- Engel, A. (1991) Biological applications of scanning sensor microscopes. *Annual Review of Biophysics and Biophysical Chemistry*, 20, 79–108.
- Foscolos, A.E., Powell, T.G., and Gunther, P.R. (1976) The use of clay minerals and inorganic and organic geochemical indicators for evaluating the degree of diagenesis and oil generating potential of shales. *Geochimica et Cosmochimica Acta*, 40, 953–966.
- Glaeser, R., and Méring, J. (1968) Domaines d'hydratation homogène des smectites. *Comptes rendus de l'Académie des Sciences à Paris*, 246, Série D, 463–466.
- Glasmann, J.R., Larter, S., Briedis, N.A., and Lundegard, P.D. (1989) Shale diagenesis in the Bergen High area. *Clays and Clay Minerals*, 37, 97–112.
- Hansen, P.L., and Lindgreen, H. (1987) Structural investigations of mixed-layer smectite-illite clay minerals from North Sea oil source rocks. In G.W. Bailey, Ed., *Proceedings of the 45th Annual Meeting of the Electron Microscopy Society of America*, Baltimore, Maryland, 1987, p. 374–375. San Francisco Press, San Francisco.
- (1989) Mixed-layer illite/smectite diagenesis in Upper Jurassic claystones from the North Sea and onshore Denmark. *Clay Minerals*, 24, 197–213.
- Hansma, P.K., and Tersoff, J. (1987) Scanning tunnelling microscopy. *Journal of Applied Physics*, 61, R1–R23.
- Hansma, P.K., Elings, V.B., Marti, O., and Bracker, C.E. (1988) Scanning tunnelling microscopy and atomic force microscopy: Application to biology and technology. *Science*, 242, 209–215.
- Hartman, H., Sposito, G., Yang, A., Manne, S., Gould, S.A.C., and Hansma, P.K. (1990) Molecular-scale imaging of clay mineral surfaces with the atomic force microscope. *Clays and Clay Minerals*, 38, 337–342.
- Holtzapffel, T., and Chamley, H. (1986) Les smectites latéites du domaine Atlantique depuis le Jurassique Supérieur: Gisement et signification. *Clay Minerals*, 21, 133–148.
- Hower, J., Eslinger, E.V., Hower, M.E., and Perry, E.A. (1976) Mechanism of burial metamorphism of argillaceous sediment: 1. Mineralogical and chemical evidence. *Geological Society of America Bulletin*, 87, 725–737.
- Lægsgaard, E., Besenbacher, F., Mortensen, K., and Stensgaard, I. (1989) A fully automated "thimble-size" scanning tunnelling microscope. *Journal of Microscopy*, 152, 663–669.
- Lindgreen, H., and Hansen, P.L. (1991) Ordering of illite/smectite in Upper Jurassic claystones from the North Sea. *Clay Minerals*, 26, 105–125.
- Lindgreen, H., Jacobsen, H., and Jakobsen, H.J. (1991) Diagenetic structure transformations in North Sea Jurassic illite/smectite. *Clays and Clay Minerals*, 39, 54–69.
- Meunier, M., Currie, J.F., Wertheimer, M.R., and Yelon, A. (1983) Electrical conduction in biotite micas. *Journal of Applied Physics*, 54, 898–905.
- Nadeau, P.H., Wilson, M.J., McHardy, W.J., and Tait, J.M. (1984) Interparticle diffraction: A new concept for interstratified clays. *Clay Minerals*, 19, 757–769.
- (1985) The conversion of smectite to illite during diagenesis: Evidence from some illitic clays from bentonites and sandstones. *Mineralogical Magazine*, 49, 393–400.
- (1987) Fundamental nature of illite/smectite: A reply. *Clays and Clay Minerals*, 35, 77–79.
- Perry, E.A., and Hower, J. (1970) Burial diagenesis in Gulf Coast pelitic sediments. *Clays and Clay Minerals*, 18, 165–177.
- Ravina, I., and Low, P.F. (1972) Relation between swelling, water properties and *b*-dimension in montmorillonite water systems. *Clays and Clay Minerals*, 20, 109–123.
- (1977) Change of *b*-dimension with swelling of montmorillonite. *Clays and Clay Minerals*, 25, 201–204.
- Reynolds, R.C. (1984) Interstratified clay minerals. In G.W. Brindley and G. Brown, Eds., *Crystal structures of clay minerals and their X-ray identification*, p. 249–303. Mineralogical Society, London.
- Weaver, C.E. (1988) *Clays, muds, and shales. Developments in sedimentology*, vol. 44, 819 p. Elsevier, Amsterdam.

MANUSCRIPT RECEIVED DECEMBER 4, 1990

MANUSCRIPT ACCEPTED APRIL 9, 1991